Electrochemical Germane (GeH_4) Synthesis via Dual-Descriptor Screening and Integrated Theoretical-Experimental Validation

Jingnan Zheng,† Jinglei Si,† Anyi Feng, Hanxiao Liu, Shijie Zhang* and Jianguo Wang**

[a]Institute of Industrial Catalysis, State Key Laboratory Breeding Base of Green-Chemical Synthesis Technology, College of Chemical Engineering, Zhejiang University of Technology, Hangzhou 310032, People's Republic of China.

[b]Zhejiang Key Laboratory of Surface and Interface Science and Engineering for Catalysts, Zhejiang University of Technology, Hangzhou 310032, People's Republic of China.

Jingnan Zheng and Jinglei Si contribute to this work equally.

Correspondence and requests for materials should be addressed to J.G.W. (email: jgw@zjut.edu.cn), Shijie Zhang (email: shijiez@zjut.edu.cn) and Jingnan Zheng (email: zhengjn0814@zjut.edu.cn).

Experimental methods

Materials

Copper (Cu), bismuth (Bi), and nickel (Ni) electrodes were supplied by Wenghou Metal Materials Co., Ltd. (Hefei, China). The mixed metal oxide (MMO, IrO_2-Ta_2O_5/Ti) anode was procured from Shuertai Co. (Suzhou, China). A proton exchange membrane was sourced from THINKRE GROUP CO., Ltd. (Suzhou, China). Germanium oxide (GeO_2, 99.99%) and sulfuric acid (H_2SO_4, GR grade) were obtained from Macklin Biochemical Co., Ltd. and Sinopharm Chemical Reagent Co., Ltd., respectively. Aqueous solutions were prepared using deionized water (Millipore, 18.2 MΩ·cm). All materials were used as received without further purification.

Table S1. Calculation and selection of surface energy of different metal sections (eV).

	001	100	110	111	Reference	Facet
Cu	0.1444	0.1437	0.1498	0.1331	111	111
Ag	0.0853	0.0853	0.0911	0.0812	111	111
Zn	0.0513	0.0705	0.0838	0.0841	001	001
Cd	0.0334	0.0518	0.0515	0.0436	001	001
Tl	0.0292	0.0272	0.0296	0.0305	/	100
Bi	0.0367	0.0287	0.0299	0.0483	111	100
Pt	0.1816	0.2005	0.1969	0.1816	111	111
Pd	0.1093	0.1093	0.1062	0.1052	111	111
Rh	0.1287	0.1287	0.1354	0.1031	111	111
Ni	0.1943	0.1943	0.1817	0.1894	111	111

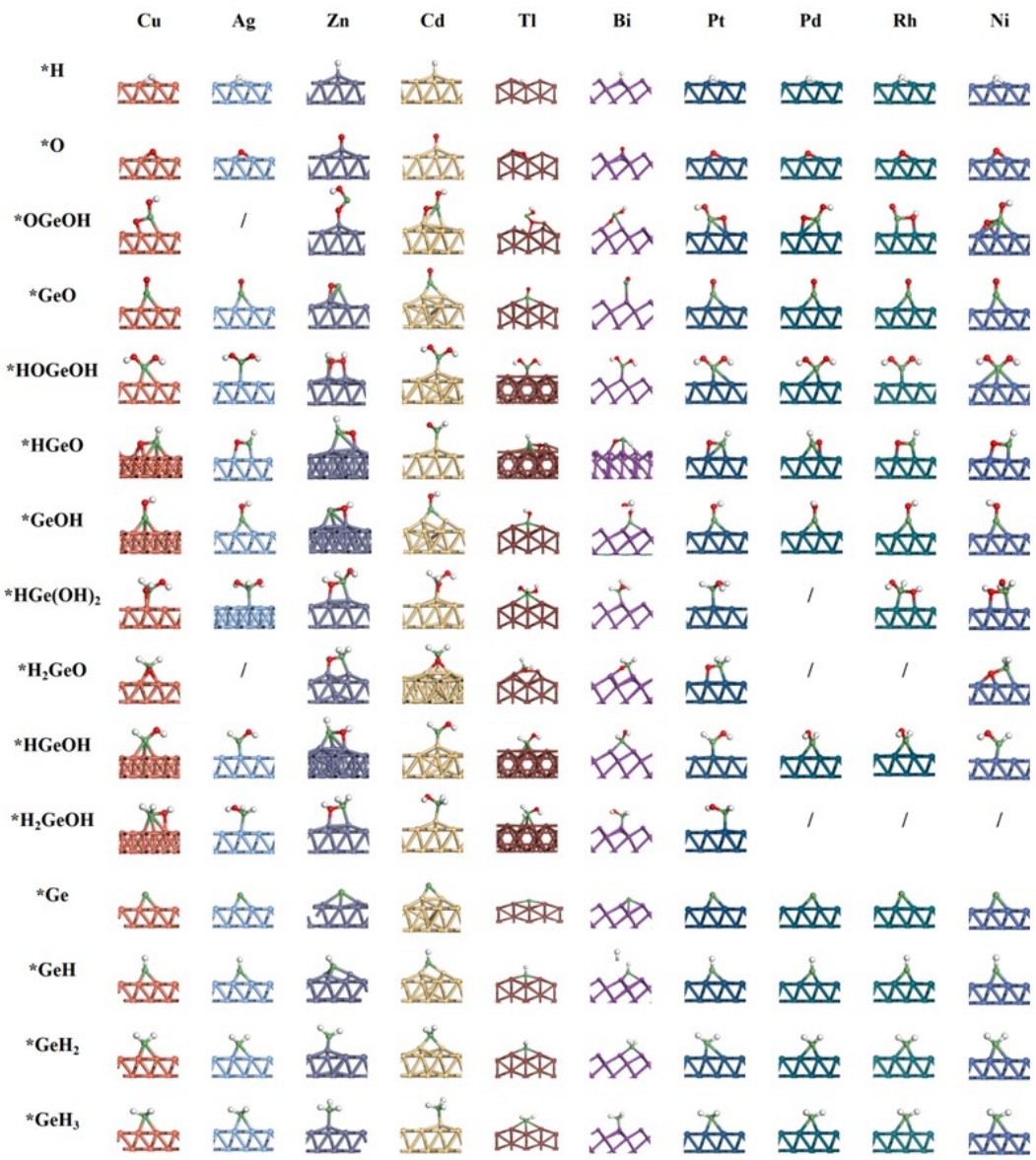

Figure S1. Structures of intermediates adsorbed on different metal surfaces.

Table S2. Energies of intermediate adsorption on different metal surfaces.

E_{ad}/eV	Cu	Ag	Zn	Cd	Tl	Bi	Pt	Pd	Rh	Ni
*H	-0.05	0.46	0.59	0.71	0.78	0.63	-0.32	-0.43	-0.35	-0.41
*O	1.03	1.54	1.67	1.79	1.86	1.89	0.76	0.65	0.73	-0.61
*OGeOH	-2.03	/	-2.13	-1.82	-2.10	-1.82	-2.69	-2.65	-2.95	-2.84
*GeO	-0.55	0.03	-0.40	0.44	-0.07	0.39	-1.65	-1.69	-1.54	-1.35
*HOGeOH	-0.48	-0.06	0.14	0.23	0.04	-0.03	-1.71	-1.58	-1.48	-1.26
*HGeO	-2.70	-2.03	-2.47	-1.84	-2.33	-2.13	-3.63	-3.52	-3.84	-3.50
*GeOH	-1.59	-0.91	-1.09	-0.95	-1.02	-1.20	-3.29	-3.25	-3.16	-2.74
*$HGe(OH)_2$	-1.39	-0.95	-1.34	-1.26	-0.92	-1.08	-2.07	/	-2.18	-1.95
*H_2GeO	-1.27	/	-1.22	-1.21	-1.00	-1.07	-1.63	/	/	/
*HGeOH	-1.00	-0.41	-0.42	-0.41	-0.42	-0.52	-2.37	-2.16	-2.09	-1.82
*H_2GeOH	-1.34	-0.91	-1.27	-1.07	-0.78	-1.08	-2.06	/	/	/
*Ge	0.28	1.02	0.91	0.98	0.99	0.75	-1.58	-1.38	-1.20	-0.80
*GeH	-2.26	-1.54	-1.81	-1.74	-1.63	-1.65	-4.02	-3.82	-3.82	-3.39
*GeH_2	-1.50	-0.93	-1.09	-1.16	-1.09	-1.37	-2.84	-2.60	-2.59	-2.27
*GeH_3	-1.67	-1.31	-1.56	-1.53	-1.26	-1.50	-2.09	-2.14	-2.00	-2.14

The adsorption energies are given in eV. A slash (/) indicates that the corresponding structure was unstable during optimization or converged to an unreasonable configuration.

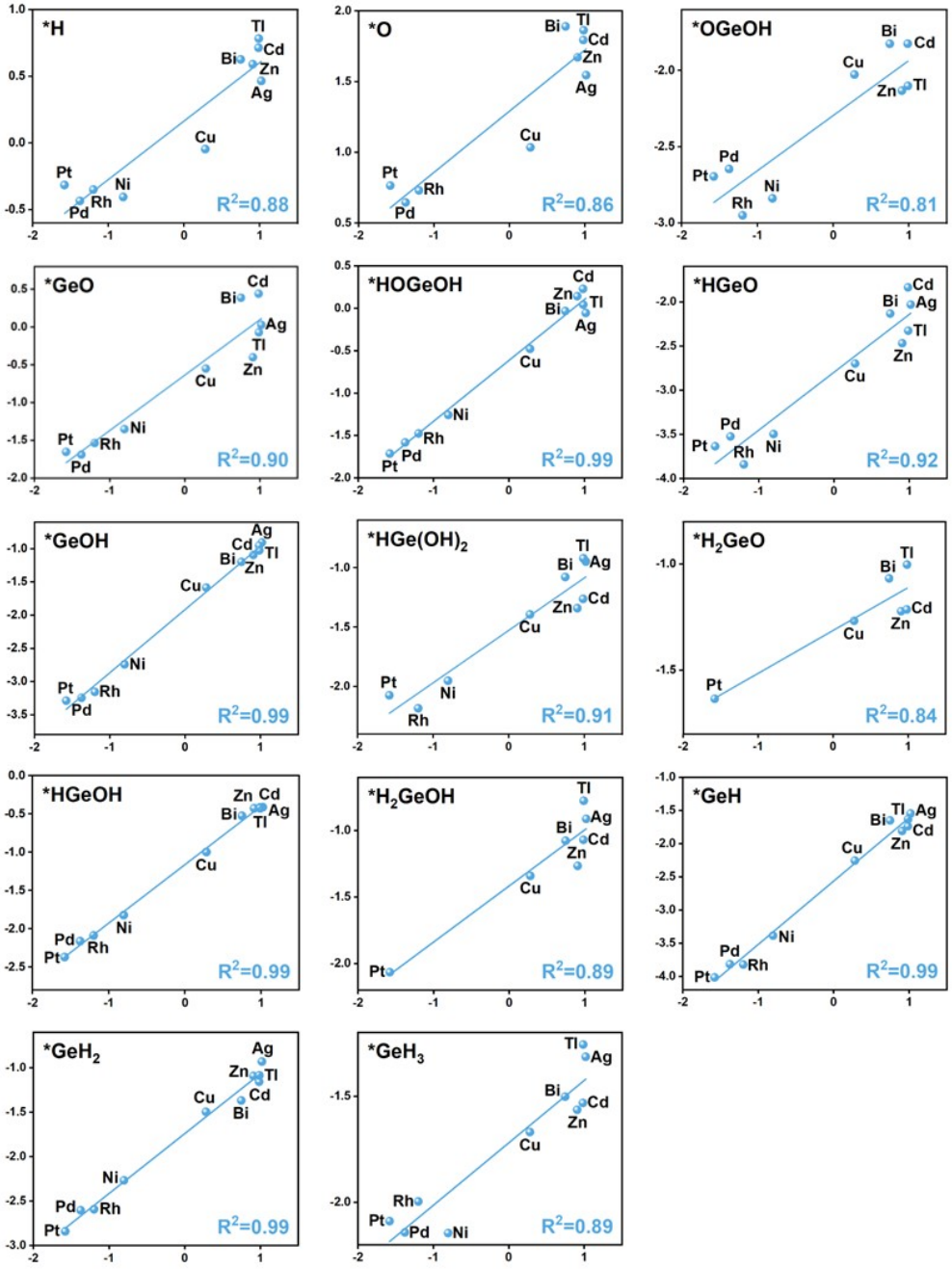

Figure S2. Linear scaling relationship between the adsorption energy of involved intermediates (vertical axis) and the germanium binding energy (horizontal axis).

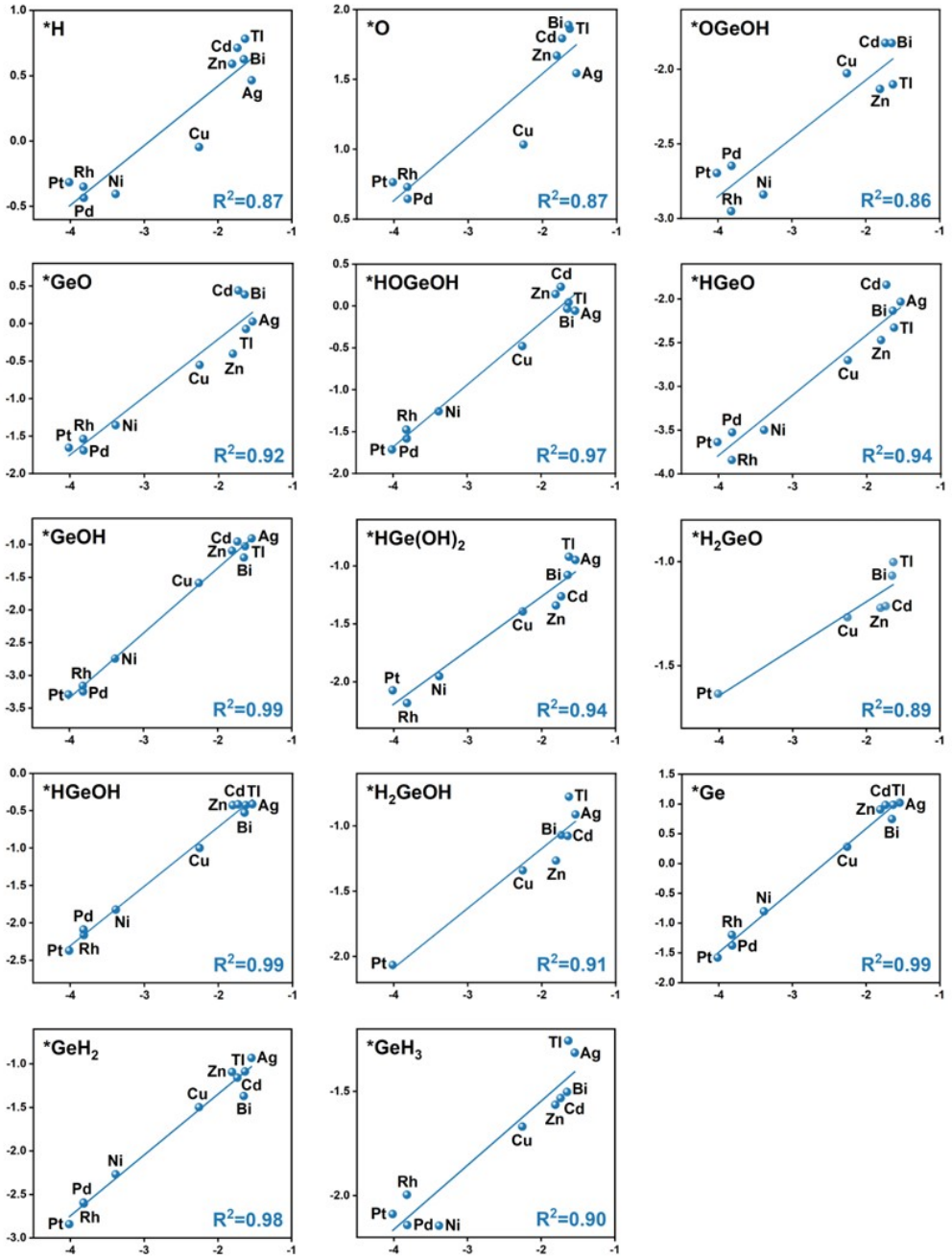

Figure S3. Linear scaling relationship between the adsorption energy of involved intermediates (vertical axis) and the GeH binding energy (horizontal axis).

Table S3. Hydrolysis-first pathways.

		Tafel-type	Heyrovsky-type
Dissociative pathway		$H^+ + e^- \rightarrow *H$ $GeO_2 \rightarrow *O + *GeO$ $*GeO \rightarrow *O + *Ge$ $*Ge + *H \rightarrow *GeH$ $*GeH + *H \rightarrow *GeH_2$ $*GeH_2 + *H \rightarrow *GeH_3$ $*GeH_3 + *H \rightarrow * + GeH_4$ $*O + *H \rightarrow *OH$ $*OH + *H \rightarrow H_2O$	$GeO_2 \rightarrow *O + *GeO$ $*GeO \rightarrow *O + *Ge$ $*Ge + (H^+ + e^-) \rightarrow *GeH$ $*GeH + (H^+ + e^-) \rightarrow *GeH_2$ $*GeH_2 + (H^+ + e^-) \rightarrow *GeH_3$ $*GeH_3 + (H^+ + e^-) \rightarrow * + GeH_4$ $*O + (H^+ + e^-) \rightarrow *OH$ $*OH + (H^+ + e^-) \rightarrow H_2O$
Associative pathway	Distal-O	$H^+ + e^- \rightarrow *H$ $GeO_2 + *H \rightarrow *OGeOH$ $*OGeOH + *H \rightarrow *GeO + H_2O$ $*GeO + *H \rightarrow *GeOH$ $*GeOH + *H \rightarrow *Ge + H_2O$ $*Ge + *H \rightarrow *GeH$ $*GeH + *H \rightarrow *GeH_2$ $*GeH_2 + *H \rightarrow *GeH_3$ $*GeH_3 + *H \rightarrow * + GeH_4$	$GeO_2 + (H^+ + e^-) \rightarrow *OGeOH$ $*OGeOH + (H^+ + e^-) \rightarrow *GeO + H_2O$ $*GeO + (H^+ + e^-) \rightarrow *GeOH$ $*GeOH + (H^+ + e^-) \rightarrow *Ge + H_2O$ $*Ge + (H^+ + e^-) \rightarrow *GeH$ $*GeH + (H^+ + e^-) \rightarrow *GeH_2$ $*GeH_2 + (H^+ + e^-) \rightarrow *GeH_3$ $*GeH_3 + (H^+ + e^-) \rightarrow * + GeH_4$
	Distal-Ge	$H^+ + e^- \rightarrow *H$ $GeO_2 + *H \rightarrow *OGeOH$ $*OGeOH + *H \rightarrow *GeO + H_2O$ $*GeO + *H \rightarrow *HGeO$ $*HGeO + *H \rightarrow *H_2GeO$ $*H_2GeO + *H \rightarrow *H_2GeOH$ $*H_2GeOH + *H \rightarrow *GeH_2$ $*GeH_2 + *H \rightarrow *GeH_3$ $*GeH_3 + *H \rightarrow * + GeH_4$	$GeO_2 + (H^+ + e^-) \rightarrow *OGeOH$ $*OGeOH + (H^+ + e^-) \rightarrow *GeO + H_2O$ $*GeO + (H^+ + e^-) \rightarrow *HGeO$ $*HGeO + (H^+ + e^-) \rightarrow *H_2GeO$ $*H_2GeO + (H^+ + e^-) \rightarrow *H_2GeOH$ $*H_2GeOH + (H^+ + e^-) \rightarrow *GeH_2$ $*GeH_2 + (H^+ + e^-) \rightarrow *GeH_3$ $*GeH_3 + (H^+ + e^-) \rightarrow * + GeH_4$
	Alternating-O	$H^+ + e^- \rightarrow *H$ $GeO_2 + *H \rightarrow *OGeOH$ $*OGeOH + *H \rightarrow *GeO + H_2O$ $*GeO + *H \rightarrow *GeOH$ $*GeOH + *H \rightarrow *HGeOH$ $*HGeOH + *H \rightarrow *H_2GeOH$ $*H_2GeOH + *H \rightarrow *GeH_2 + H_2O$ $*GeH_2 + *H \rightarrow *GeH_3$ $*GeH_3 + *H \rightarrow * + GeH_4$	$GeO_2 + (H^+ + e^-) \rightarrow *OGeOH$ $*OGeOH + (H^+ + e^-) \rightarrow *GeO + H_2O$ $*GeO + (H^+ + e^-) \rightarrow *GeOH$ $*GeOH + (H^+ + e^-) \rightarrow *HGeOH$ $*HGeOH + (H^+ + e^-) \rightarrow *H_2GeOH$ $*H_2GeOH + (H^+ + e^-) \rightarrow *GeH_2 + H_2O$ $*GeH_2 + (H^+ + e^-) \rightarrow *GeH_3$ $*GeH_3 + (H^+ + e^-) \rightarrow * + GeH_4$
		$H^+ + e^- \rightarrow *H$ $GeO_2 + *H \rightarrow *OGeOH$ $*OGeOH + *H \rightarrow *GeO + H_2O$ $*GeO + *H \rightarrow *GeOH$ $*GeOH + *H \rightarrow *HGeOH$ $*HGeOH + *H \rightarrow *GeH + H_2O$ $*GeH + *H \rightarrow *GeH_2$ $*GeH_2 + *H \rightarrow *GeH_3$ $*GeH_3 + *H \rightarrow * + GeH_4$	$GeO_2 + (H^+ + e^-) \rightarrow *OGeOH$ $*OGeOH + (H^+ + e^-) \rightarrow *GeO + H_2O$ $*GeO + (H^+ + e^-) \rightarrow *GeOH$ $*GeOH + (H^+ + e^-) \rightarrow *HGeOH$ $*HGeOH + (H^+ + e^-) \rightarrow *GeH + H_2O$ $*GeH + (H^+ + e^-) \rightarrow *GeH_2$ $*GeH_2 + (H^+ + e^-) \rightarrow *GeH_3$ $*GeH_3 + (H^+ + e^-) \rightarrow * + GeH_4$
	Alternating-Ge	$H^+ + e^- \rightarrow *H$ $GeO_2 + *H \rightarrow *OGeOH$ $*OGeOH + *H \rightarrow *GeO + H_2O$ $*GeO + *H \rightarrow *HGeO$ $*HGeO + *H \rightarrow *HGeOH$ $*HGeOH + *H \rightarrow *H_2GeOH$ $*H_2GeOH + *H \rightarrow *GeH_2 + H_2O$ $*GeH_2 + *H \rightarrow *GeH_3$ $*GeH_3 + *H \rightarrow * + GeH_4$	$GeO_2 + (H^+ + e^-) \rightarrow *OGeOH$ $*OGeOH + (H^+ + e^-) \rightarrow *GeO + H_2O$ $*GeO + (H^+ + e^-) \rightarrow *HGeO$ $*HGeO + (H^+ + e^-) \rightarrow *HGeOH$ $*HGeOH + (H^+ + e^-) \rightarrow *H_2GeOH$ $*H_2GeOH + (H^+ + e^-) \rightarrow *GeH_2 + H_2O$ $*GeH_2 + (H^+ + e^-) \rightarrow *GeH_3$ $*GeH_3 + (H^+ + e^-) \rightarrow * + GeH_4$
		$H^+ + e^- \rightarrow *H$ $GeO_2 + *H \rightarrow *OGeOH$ $*OGeOH + *H \rightarrow *GeO + H_2O$ $*GeO + *H \rightarrow *HGeO$ $*HGeO + *H \rightarrow *HGeOH$ $*HGeOH + *H \rightarrow *GeH + H_2O$ $*GeH + *H \rightarrow *GeH_2$ $*GeH_2 + *H \rightarrow *GeH_3$ $*GeH_3 + *H \rightarrow * + GeH_4$	$GeO_2 + (H^+ + e^-) \rightarrow *OGeOH$ $*OGeOH + (H^+ + e^-) \rightarrow *GeO + H_2O$ $*GeO + (H^+ + e^-) \rightarrow *HGeO$ $*HGeO + (H^+ + e^-) \rightarrow *HGeOH$ $*HGeOH + (H^+ + e^-) \rightarrow *GeH + H_2O$ $*GeH + (H^+ + e^-) \rightarrow *GeH_2$ $*GeH_2 + (H^+ + e^-) \rightarrow *GeH_3$ $*GeH_3 + (H^+ + e^-) \rightarrow * + GeH_4$

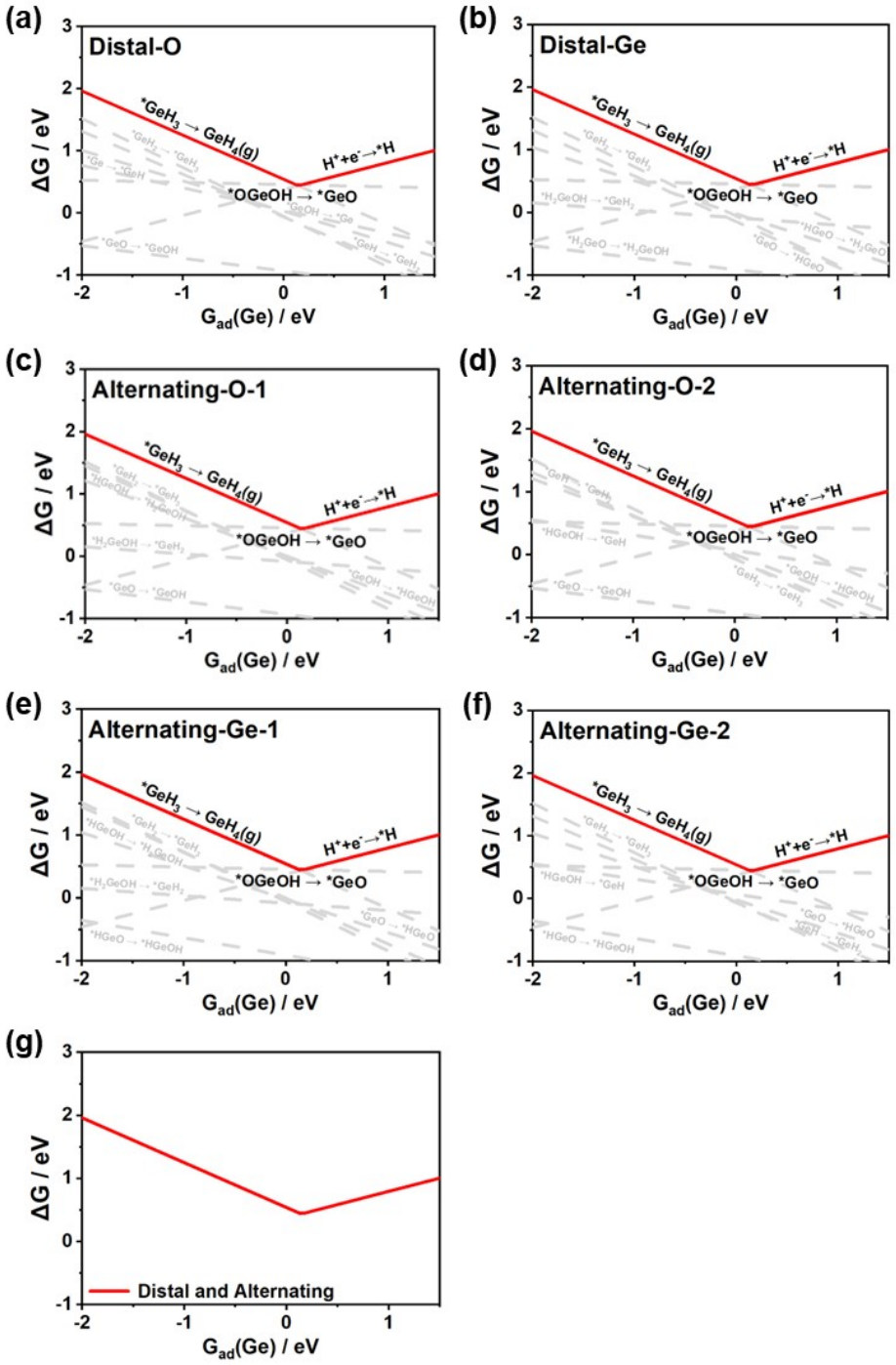

Figure S4. Reaction free energy (ΔG) of elementary reactions plotted as G_{ad}(Ge) for A-T mechanism of the hydrolysis-first pathway. (a) distal-O, (b) distal-Ge, (c) alternating-O-1, (d) alternating-O-2, (e) alternating-Ge-1 and (f) alternating-Ge-2 pathway. The red solid lines in (a)-(f) are the GDS. (g) Compaison of the GDS in different pathways.

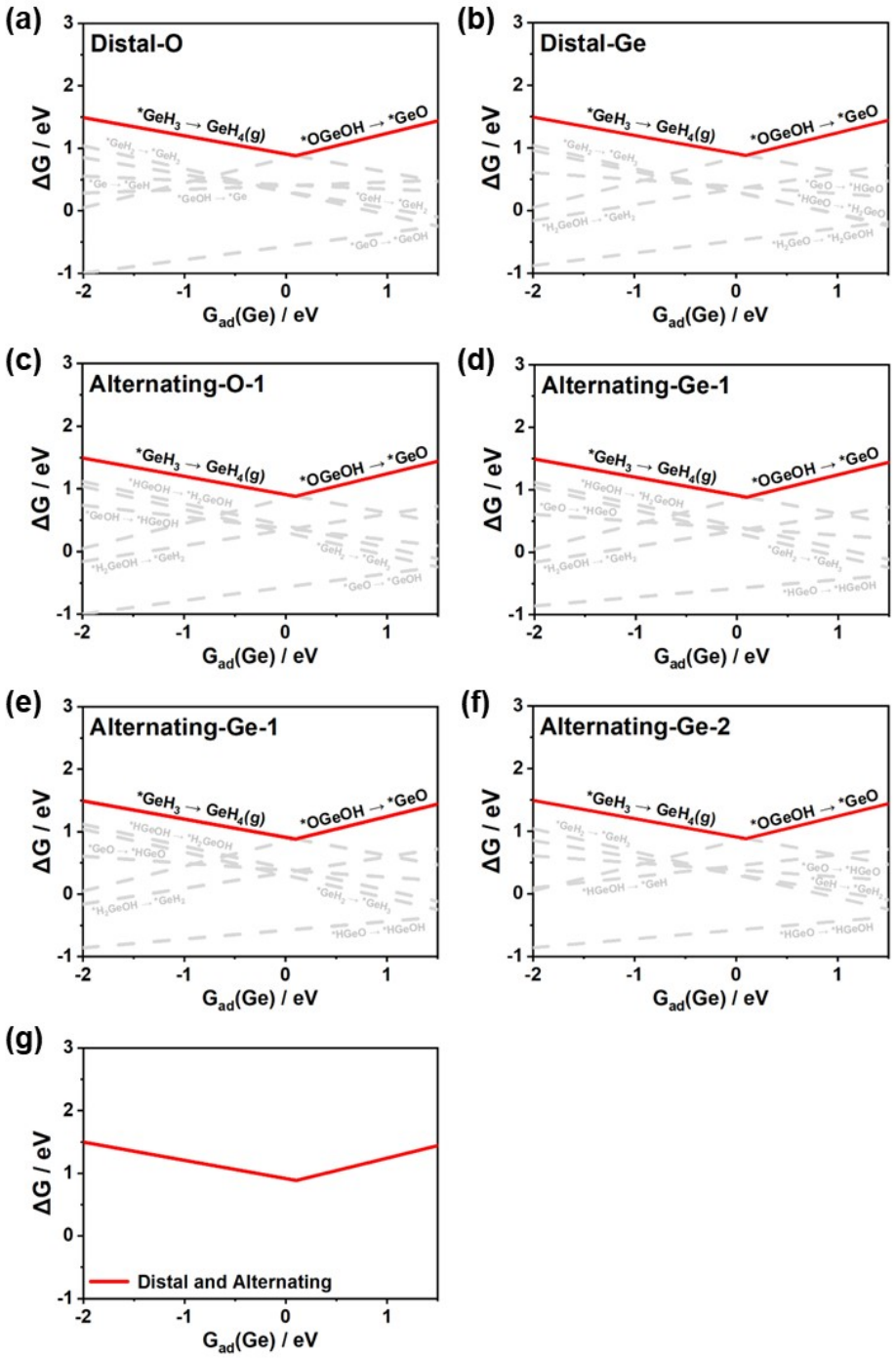

Figure S5. Reaction free energy (ΔG) of elementary reactions plotted as G_{ad}(Ge) for A-H mechanism of the hydrolysis-first pathway. (a) distal-O, (b) distal-Ge, (c) alternating-O-1, (d) alternating-O-2, (e) alternating-Ge-1 and (f) alternating- Ge-2 pathway. The red solid lines in (a)-(f) are the GDS. (g) Compaison of the GDS in different pathways.

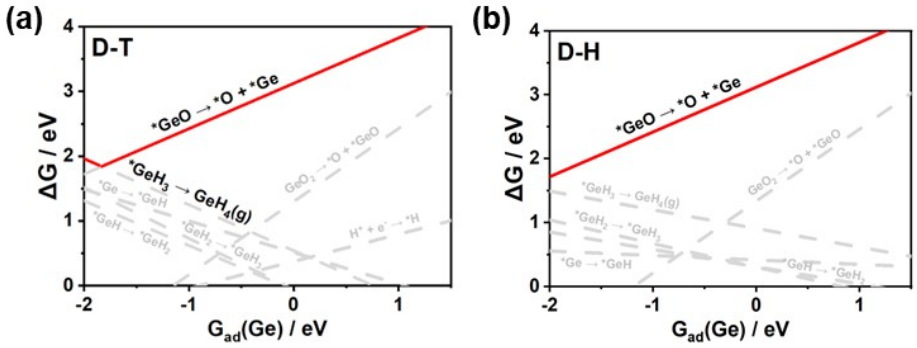

Figure S6. Reaction free energy (ΔG) of elementary reactions plotted as G_{ad}(Ge) for D-T (a) and D-H (b) mechanism of the hydrolysis-first pathway. The red solid lines represent the GDS.

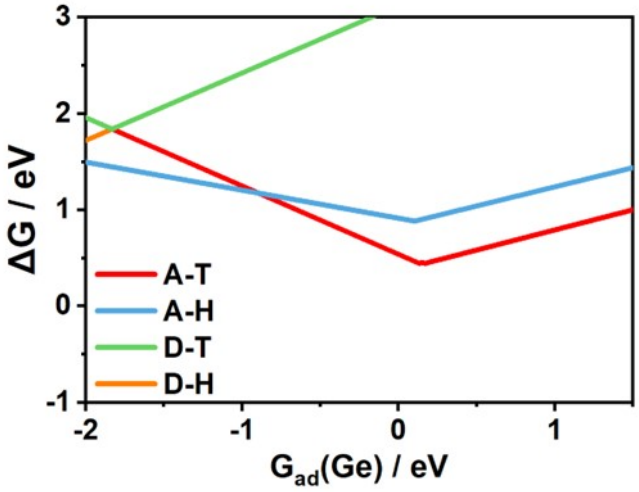

Figure S7. Comparison of GDS between different mechanisms of the hydrolysis-first pathway based on the G_{ad}(Ge) descriptor.

Table S4. Non-hydrolysis-first pathways.

		Tafel-type	Heyrovsky-type
Dissociative pathway		$H^+ + e^- \rightarrow *H$ $GeO_2 + *H \rightarrow *OGeOH$ $*OGeOH + *H \rightarrow *HOGeOH$ $*HOGeOH + *H \rightarrow *GeOH + H_2O$ $*GeOH + *H \rightarrow *Ge + H_2O$ $*Ge + *H \rightarrow *GeH$ $*GeH + *H \rightarrow *GeH_2$ $*GeH_2 + *H \rightarrow *GeH_3$ $*GeH_3 + *H \rightarrow * + GeH_4$	$GeO_2 + (H^+ + e^-) \rightarrow *OGeOH$ $*OGeOH + (H^+ + e^-) \rightarrow *HOGeOH$ $*HOGeOH + (H^+ + e^-) \rightarrow *GeOH + H_2O$ $*GeOH + (H^+ + e^-) \rightarrow *Ge + H_2O$ $*Ge + (H^+ + e^-) \rightarrow *GeH$ $*GeH + (H^+ + e^-) \rightarrow *GeH_2$ $*GeH_2 + (H^+ + e^-) \rightarrow *GeH_3$ $*GeH_3 + (H^+ + e^-) \rightarrow * + GeH_4$
Associative pathway	Alternating-O	$H^+ + e^- \rightarrow *H$ $GeO_2 + *H \rightarrow *OGeOH$ $*OGeOH + *H \rightarrow *HOGeOH$ $*HOGeOH + *H \rightarrow *GeOH + H_2O$ $*GeOH + *H \rightarrow *HGeOH$ $*HGeOH + *H \rightarrow *H_2GeOH$ $*H_2GeOH + *H \rightarrow *GeH_2 + H_2O$ $*GeH_2 + *H \rightarrow *GeH_3$ $*GeH_3 + *H \rightarrow * + GeH_4$	$GeO_2 + (H^+ + e^-) \rightarrow *OGeOH$ $*OGeOH + (H^+ + e^-) \rightarrow *HOGeOH$ $*HOGeOH + (H^+ + e^-) \rightarrow *GeOH + H_2O$ $*GeOH + (H^+ + e^-) \rightarrow *HGeOH$ $*HGeOH + (H^+ + e^-) \rightarrow *H_2GeOH$ $*H_2GeOH + (H^+ + e^-) \rightarrow *GeH_2 + H_2O$ $*GeH_2 + (H^+ + e^-) \rightarrow *GeH_3$ $*GeH_3 + (H^+ + e^-) \rightarrow * + GeH_4$
		$H^+ + e^- \rightarrow *H$ $GeO_2 + *H \rightarrow *OGeOH$ $*OGeOH + *H \rightarrow *HOGeOH$ $*HOGeOH + *H \rightarrow *GeOH + H_2O$ $*GeOH + *H \rightarrow *HGeOH$ $*HGeOH + *H \rightarrow *GeH + H_2O$ $*GeH + *H \rightarrow *GeH_2$ $*GeH_2 + *H \rightarrow *GeH_3$ $*GeH_3 + *H \rightarrow * + GeH_4$	$GeO_2 + (H^+ + e^-) \rightarrow *OGeOH$ $*OGeOH + (H^+ + e^-) \rightarrow *HOGeOH$ $*HOGeOH + (H^+ + e^-) \rightarrow *GeOH + H_2O$ $*GeOH + (H^+ + e^-) \rightarrow *HGeOH$ $*HGeOH + (H^+ + e^-) \rightarrow *GeH + H_2O$ $*GeH + (H^+ + e^-) \rightarrow *GeH_2$ $*GeH_2 + (H^+ + e^-) \rightarrow *GeH_3$ $*GeH_3 + (H^+ + e^-) \rightarrow * + GeH_4$
	Alternating-Ge	$H^+ + e^- \rightarrow *H$ $GeO_2 + *H \rightarrow *OGeOH$ $*OGeOH + *H \rightarrow *HOGeOH$ $*HOGeOH + *H \rightarrow *HGe(OH)_2$ $*HGe(OH)_2 + *H \rightarrow *HGeOH + H_2O$ $*HGeOH + *H \rightarrow *H_2GeOH$ $*H_2GeOH + *H \rightarrow *GeH_2 + H_2O$ $*GeH_2 + *H \rightarrow *GeH_3$ $*GeH_3 + *H \rightarrow * + GeH_4$	$GeO_2 + (H^+ + e^-) \rightarrow *OGeOH$ $*OGeOH + (H^+ + e^-) \rightarrow *HOGeOH$ $*HOGeOH + (H^+ + e^-) \rightarrow *HGe(OH)_2$ $*HGe(OH)_2 + (H^+ + e^-) \rightarrow *HGeOH + H_2O$ $*HGeOH + (H^+ + e^-) \rightarrow *H_2GeOH$ $*H_2GeOH + (H^+ + e^-) \rightarrow *GeH_2 + H_2O$ $*GeH_2 + (H^+ + e^-) \rightarrow *GeH_3$ $*GeH_3 + (H^+ + e^-) \rightarrow * + GeH_4$
		$H^+ + e^- \rightarrow *H$ $GeO_2 + *H \rightarrow *OGeOH$ $*OGeOH + *H \rightarrow *HOGeOH$ $*HOGeOH + *H \rightarrow *HGe(OH)_2$ $*HGe(OH)_2 + *H \rightarrow *HGeOH + H_2O$ $*HGeOH + *H \rightarrow *GeH + H_2O$ $*GeH + *H \rightarrow *GeH_2$ $*GeH_2 + *H \rightarrow *GeH_3$ $*GeH_3 + *H \rightarrow * + GeH_4$	$GeO_2 + (H^+ + e^-) \rightarrow *OGeOH$ $*OGeOH + (H^+ + e^-) \rightarrow *HOGeOH$ $*HOGeOH + (H^+ + e^-) \rightarrow *HGe(OH)_2$ $*HGe(OH)_2 + (H^+ + e^-) \rightarrow *HGeOH + H_2O$ $*HGeOH + (H^+ + e^-) \rightarrow *GeH + H_2O$ $*GeH + (H^+ + e^-) \rightarrow *GeH_2$ $*GeH_2 + (H^+ + e^-) \rightarrow *GeH_3$ $*GeH_3 + (H^+ + e^-) \rightarrow * + GeH_4$

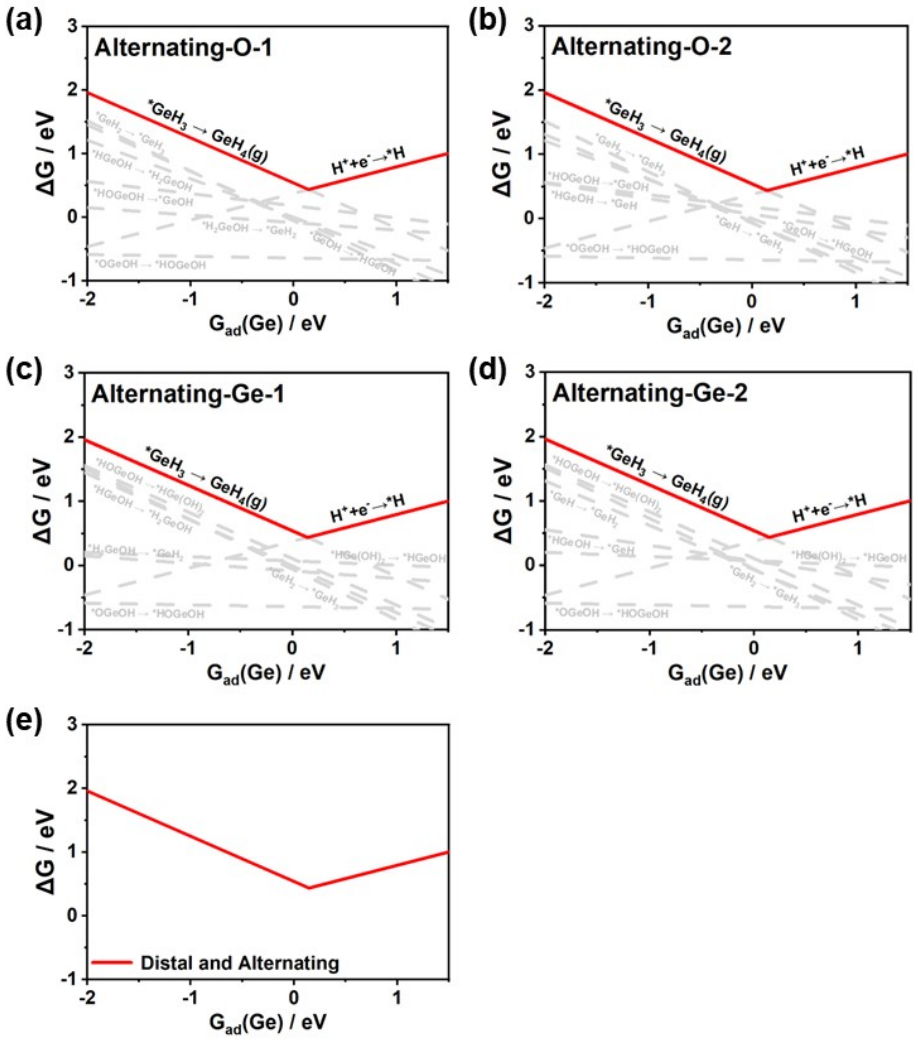

Figure S8. Reaction free energy (ΔG) of elementary reactions plotted as G_{ad}(Ge) for A-H mechanism of the non-hydrolysis-first pathway. (a) alternating-O-1, (b) alternating-O-2, (c) alternating-Ge-1 and (d) alternating-Ge-2 pathway. The red solid lines in (a)-(d) are the GDS. (e) Compaison of the GDS in different pathways.

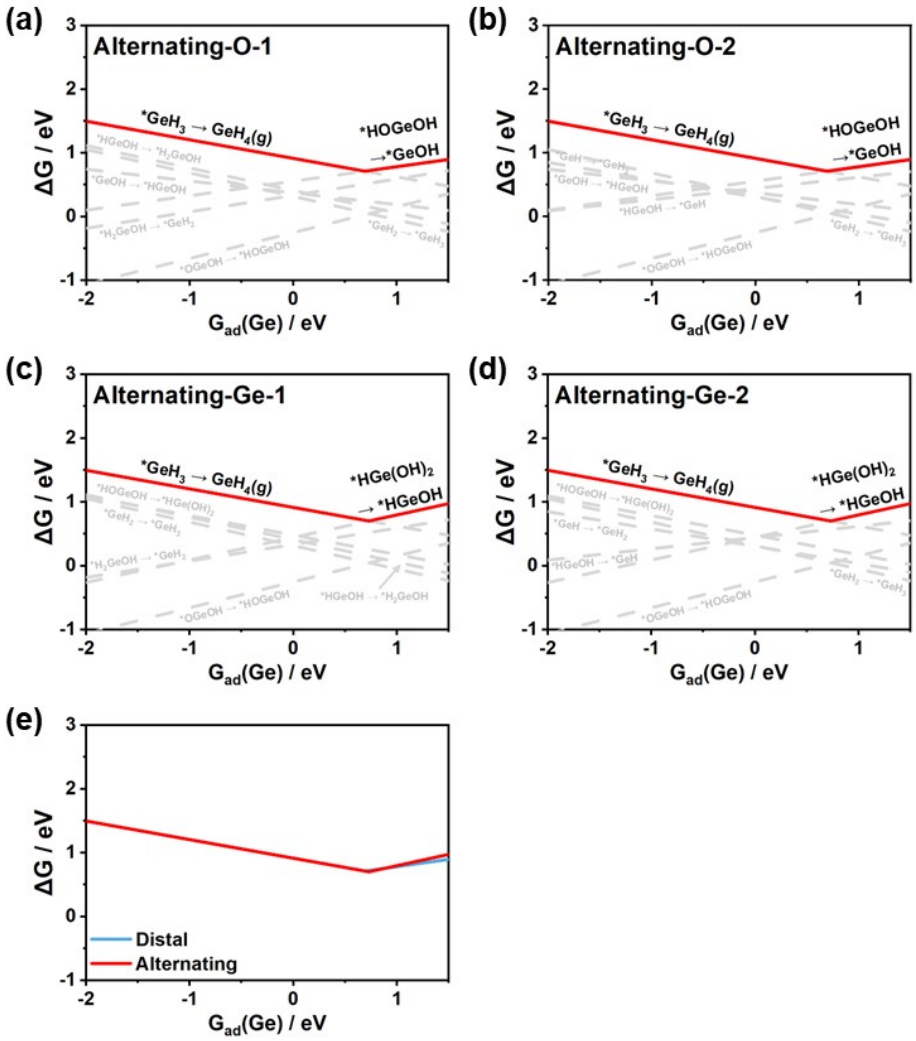

Figure S9. Reaction free energy (ΔG) of elementary reactions plotted as G_{ad}(Ge) for A-H mechanism of the non-hydrolysis-first pathway. (a) alternating-O-1, (b) alternating-O-2, (c) alternating-Ge-1 and (d) alternating-Ge-2 pathway. The red solid lines in (a)-(d) are the GDS. (e) Compaison of the GDS in different pathways.

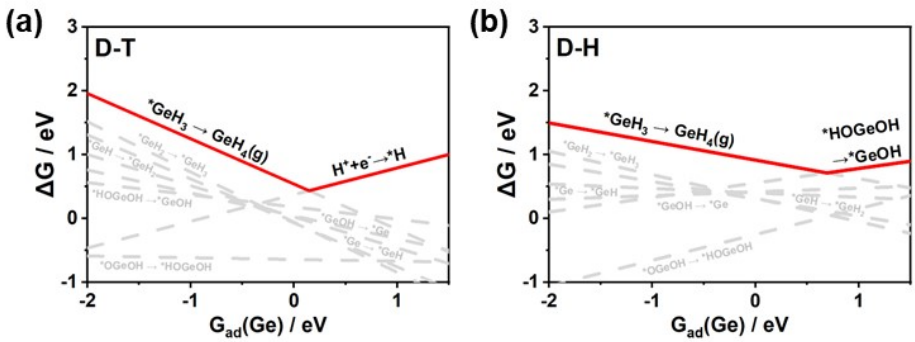

Figure S10. Reaction free energy (ΔG) of elementary reactions plotted as G_{ad}(Ge) for D-T (a) and D-H (b) mechanism of the non-hydrolysis-first pathway. The red solid lines represent the GDS.

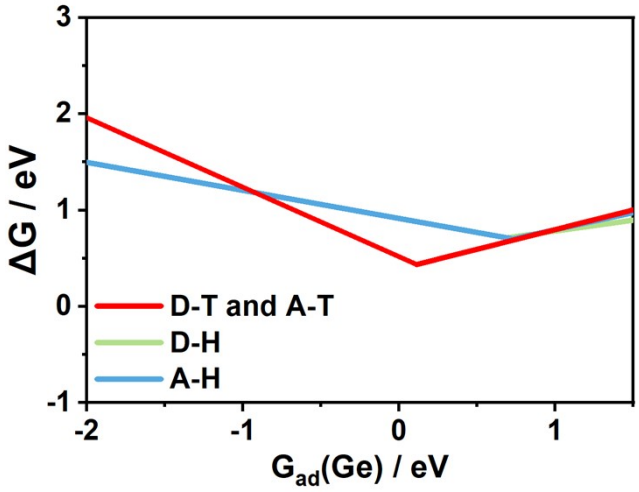

Figure S11. Comparison of GDS between different mechanisms of the non-hydrolysis-first pathway based on the G_{ad}(Ge) descriptor.

Both G_{ad}(Ge) and G_{ad}(GeH) are employed as dual descriptors to capture oxide-derived and hydride-derived chemistries in germane electrosynthesis. For conciseness, the main text presents the analysis based on G_{ad}(Ge) as an example, while the corresponding results obtained from G_{ad}(GeH) are provided in **Figures S12-S20**. The two descriptors lead to consistent scaling relations, Gibbs-determining steps, and thermodynamic boundaries, confirming the reliability of the descriptor framework.

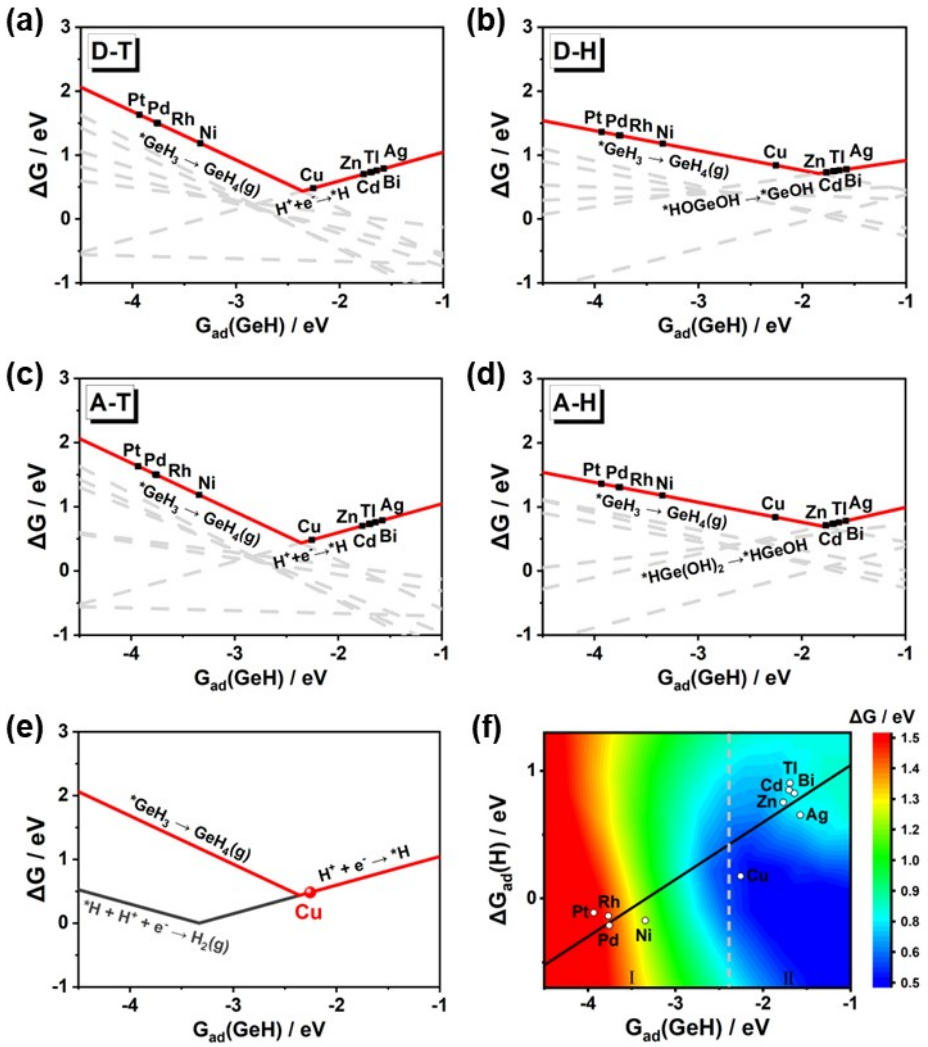

Figure S12. Linear scaling relationship between the adsorption energy of involved intermediates (vertical axis) and the GeH binding energy (horizontal axis).

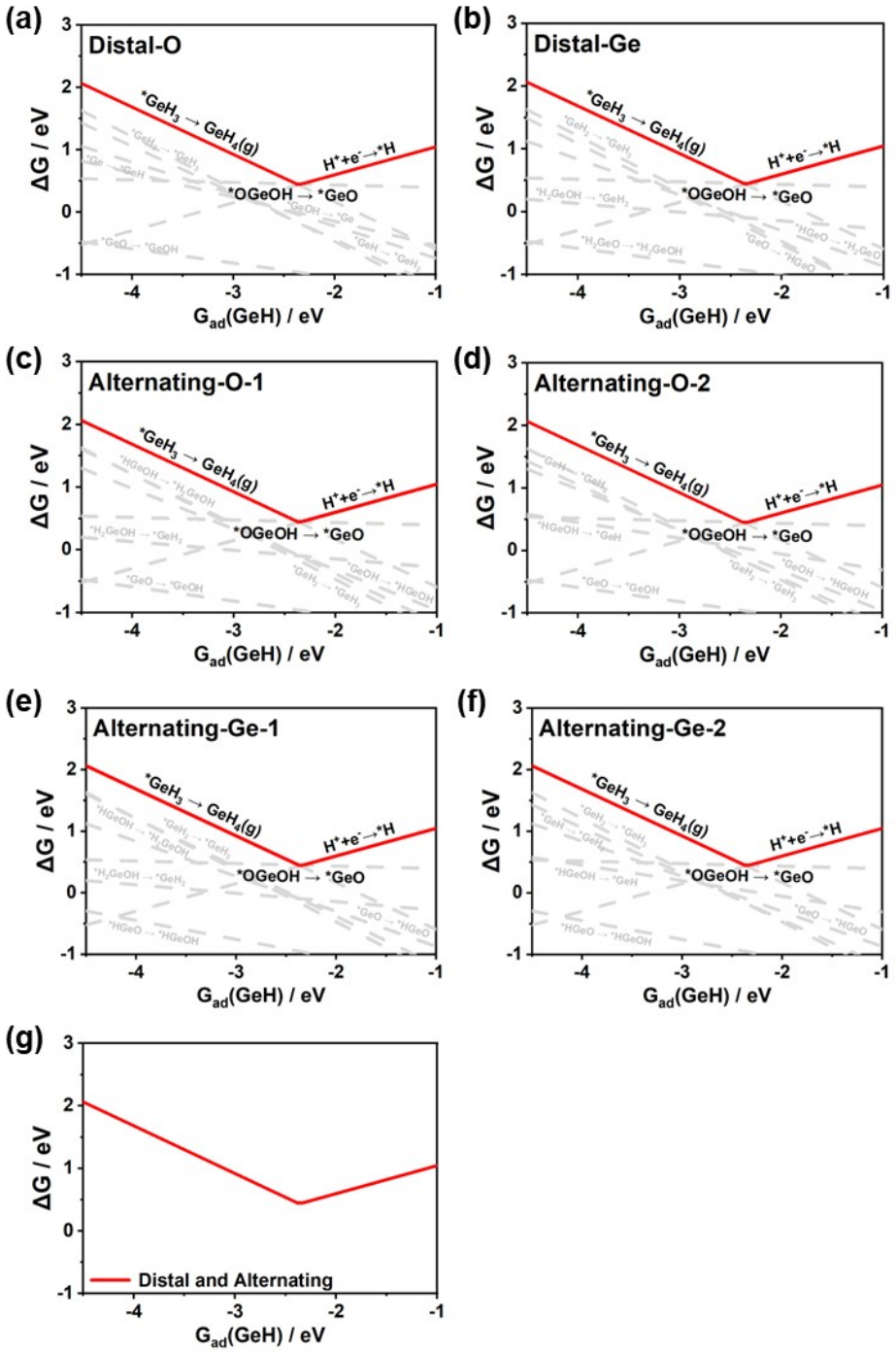

Figure S13. Reaction free energy (ΔG) of elementary reactions plotted as G_{ad}(GeH) for A-T mechanism of the hydrolysis-first pathway. (a) distal-O, (b) distal-Ge, (c) alternating-O-1, (d) alternating-O-2, (e) alternating-Ge-1 and (f) alternating-Ge-2 pathway. The red solid lines in (a)-(f) are the GDS. (g) Compaison of the GDS in different pathways.

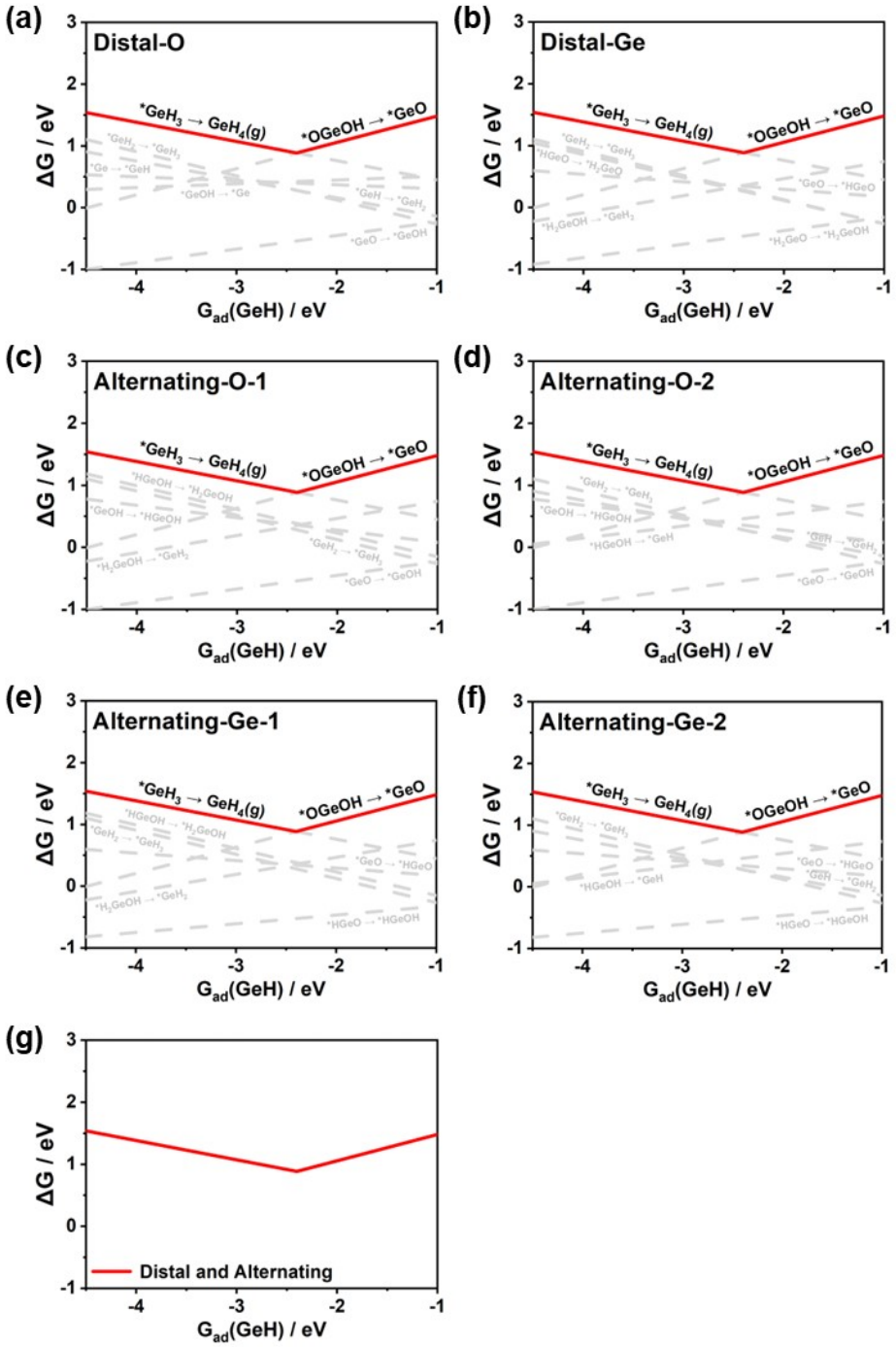

Figure S14. Reaction free energy (ΔG) of elementary reactions plotted as G_{ad}(GeH) for A-H mechanism of the hydrolysis-first pathway. (a) distal-O, (b) distal-Ge, (c) alternating-O-1, (d) alternating-O-2, (e) alternating-Ge-1 and (f) alternating-Ge-2 pathway. The red solid lines in (a)-(f) are the GDS. (g) Compaison of the GDS in different pathways.

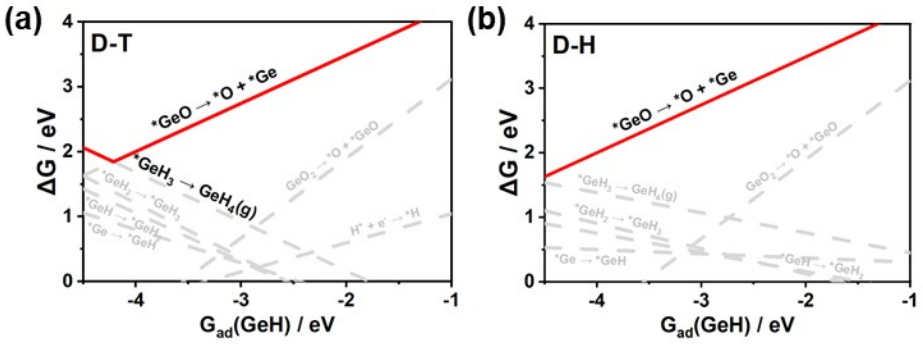

Figure S15. Reaction free energy (ΔG) of elementary reactions plotted as G_{ad}(GeH) for D-T (a) and D-H (b) mechanism of the hydrolysis-first pathway. The red solid lines represent the GDS.

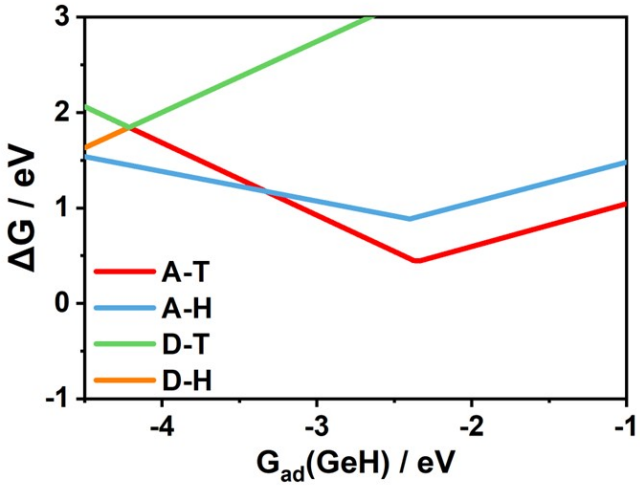

Figure S16. Comparison of GDS between different mechanisms of the hydrolysis-first pathway based on the G_{ad}(GeH) descriptor.

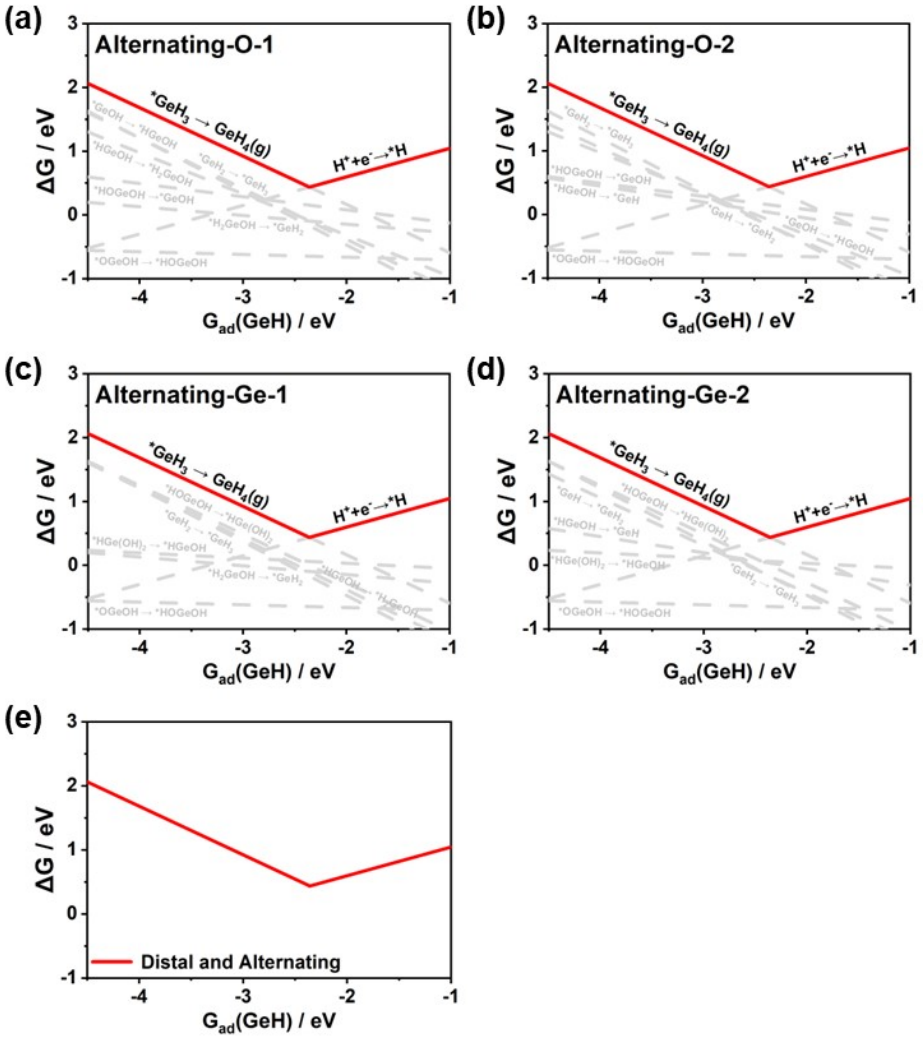

Figure S17. Reaction free energy (ΔG) of elementary reactions plotted as G_{ad}(GeH) for A-H mechanism of the non-hydrolysis-first pathway. (a) alternating-O-1, (b) alternating-O-2, (c) alternating-Ge-1 and (d) alternating-Ge-2 pathway. The red solid lines in (a)-(d) are the GDS. (e) Compaison of the GDS in different pathways.

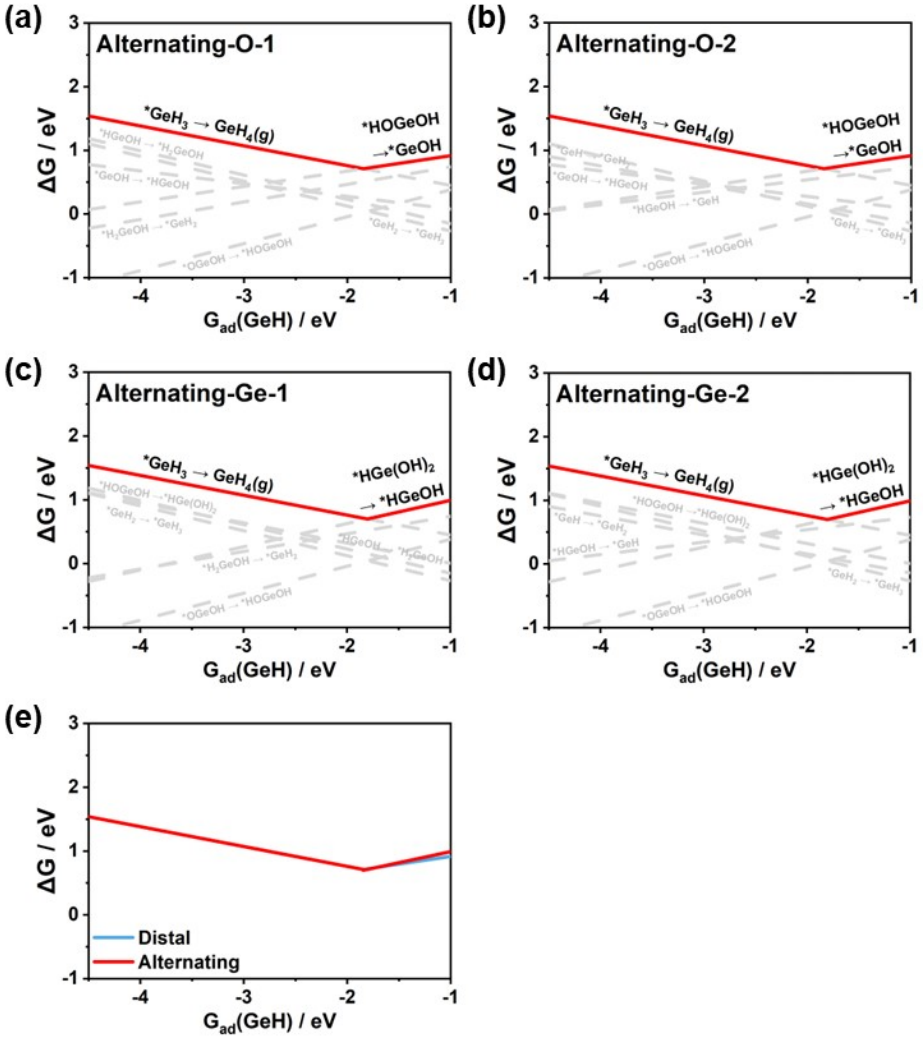

Figure S18. Reaction free energy (ΔG) of elementary reactions plotted as G_{ad}(GeH) for A-H mechanism of the non-hydrolysis-first pathway. (a) alternating-O-1, (b) alternating-O-2, (c) alternating-Ge-1 and (d) alternating-Ge-2 pathway. The red solid lines in (a)-(d) are the GDS. (e) Compaison of the GDS in different pathways.

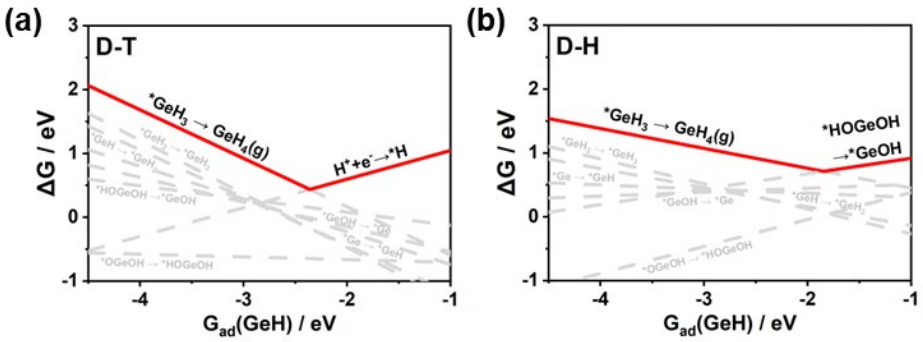

Figure S19. Reaction free energy (ΔG) of elementary reactions plotted as G_{ad}(GeH) for D-T (a) and D-H (b) mechanism of the non-hydrolysis-first pathway. The red solid lines represent the GDS.

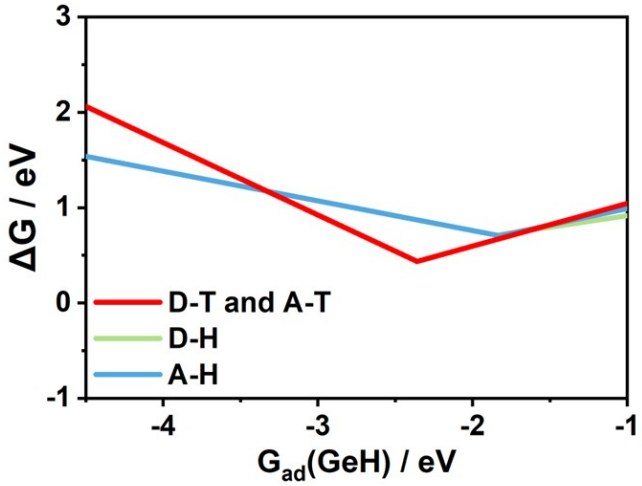

Figure S20. Comparison of GDS between different mechanisms of the non-hydrolysis-first pathway based on the G_{ad}(GeH) descriptor.

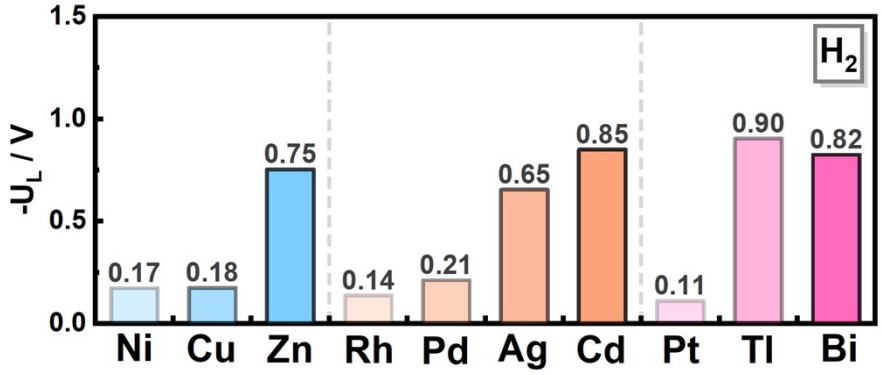

Figure S21. The limiting potential of hydrogen evolution reaction for different metals.

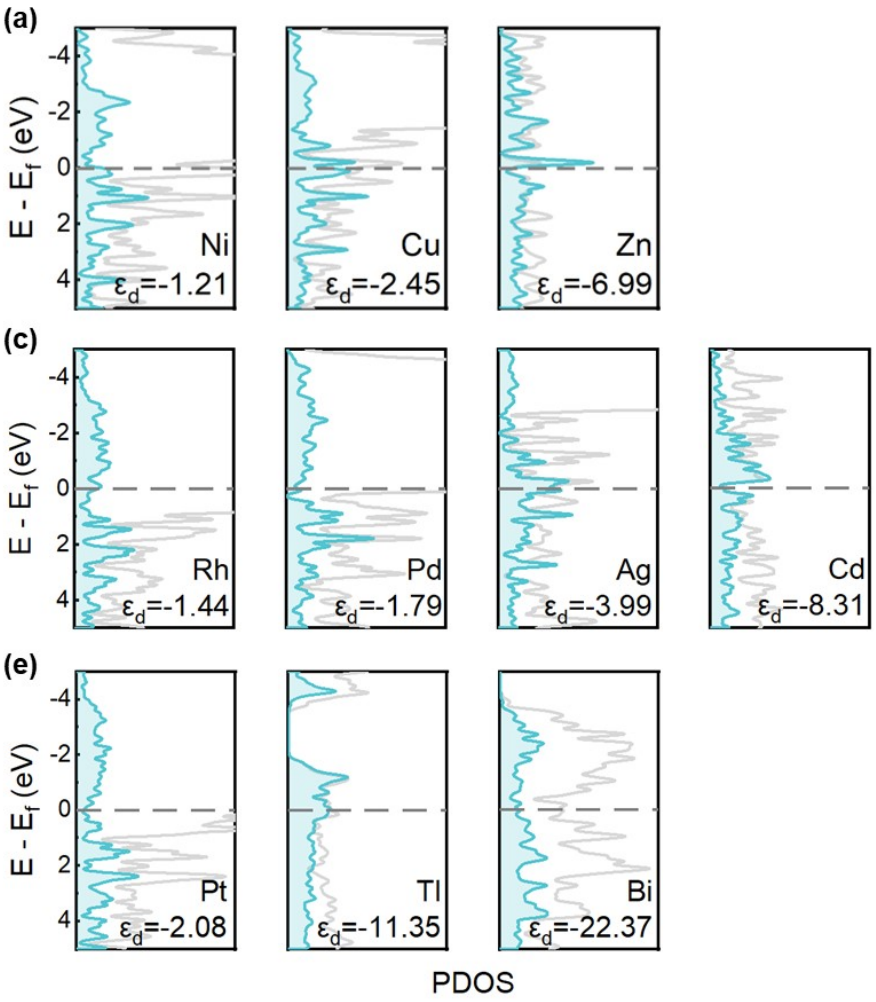

Figure S22. Partial density of states (PDOS) and d-band center of Ge atoms adsorbed on (a) 3d metals (Ni, Cu, Zn), (b) 4d metals (Rh, Pd, Ag, Cd), and (c) 5d metals (Pt, Au, Tl, Bi) surfaces. The cyan and gray regions represent the Ge p orbitals and the metal d orbitals, respectively.

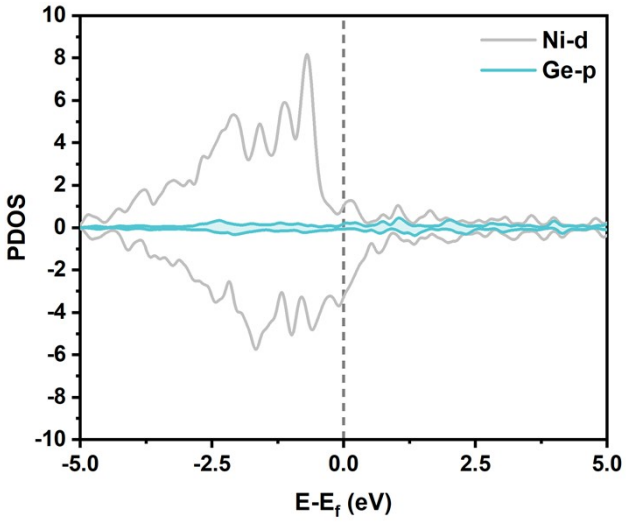

Figure S23. PDOS of Ge atom adsorbed on the Ni surface. The cyan and gray regions represent the Ge p orbitals and the metal d orbitals, respectively. Both spin-up and spin-down contributions are included.

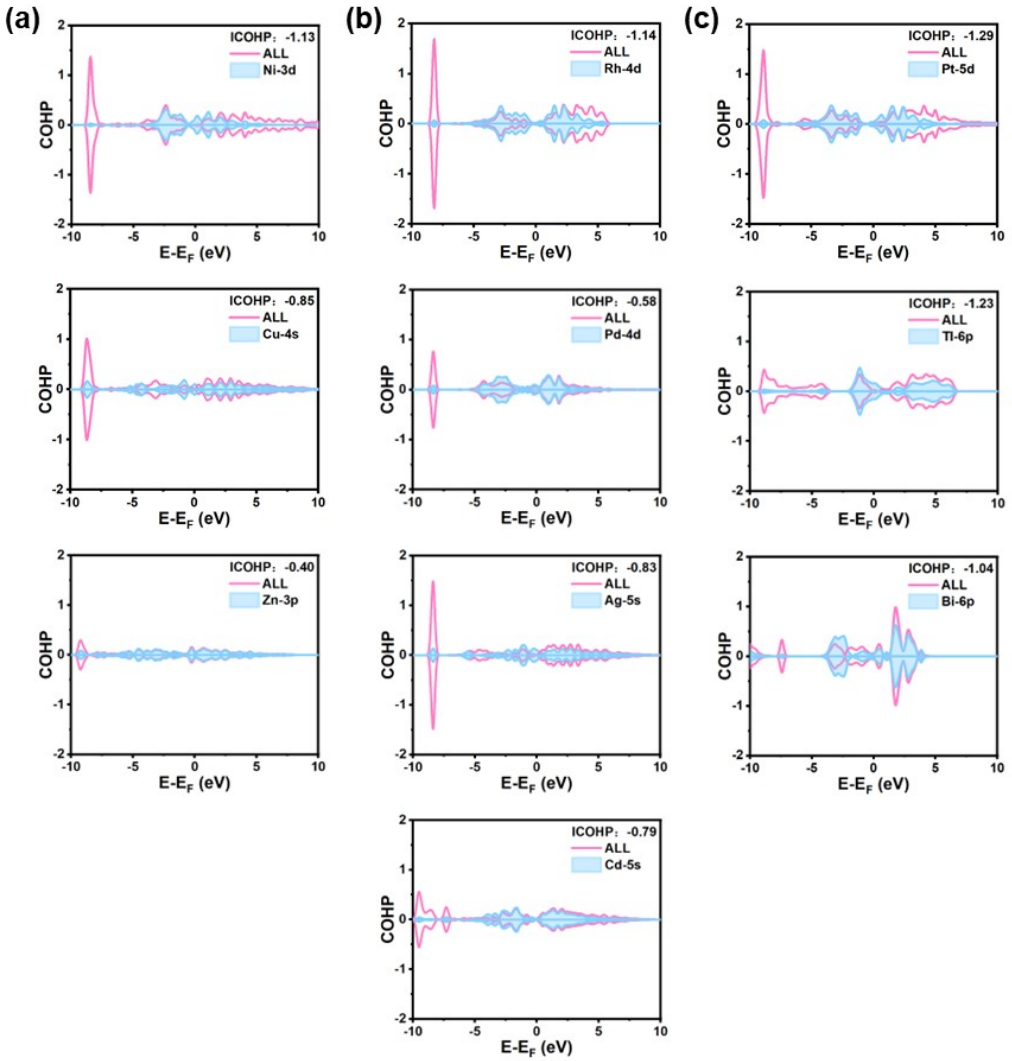

Figure S24. Integrated Crystal Orbital Hamiltonian Population below Fermi Level of Ge adsorbed on (a) 3d metals (Ni, Cu, Zn), (b) 4d metals (Rh, Pd, Ag, Cd) and (c) 5d metals (Pt, Au, Tl, Bi) surfaces.

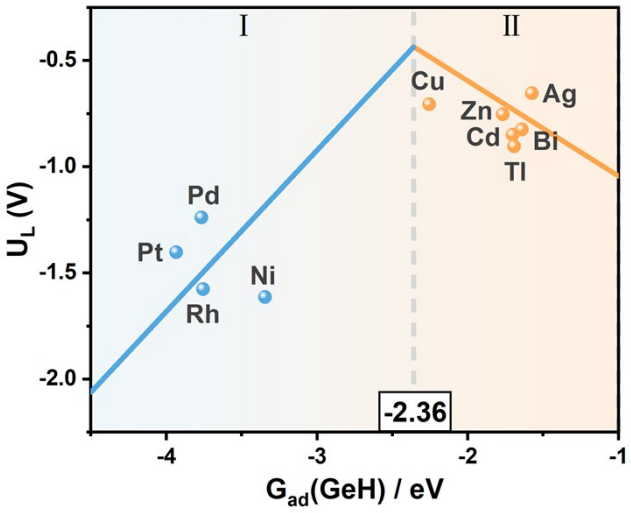

Figure S25. Volcano-type relationship between theoretical limiting potential (U_L) and GeH adsorption free energy (G_{ad}(GeH)) across different metal surfaces.

Table S5. Hydrogen adsorption free energies on Ge and Bi surfaces (eV).

	$E_{slab+adsorbate}$	E_{ZEP}	S	$G_{slab+adsorbate}$	G_{H2}	G_{slab}	$G_{ad}(H)$
Ge	-287.90	0.19	0.00	-287.72	-3.55	-284.16	-0.01
Bi	-246.86	0.15	0.00	-246.73	-3.55	-244.00	0.82

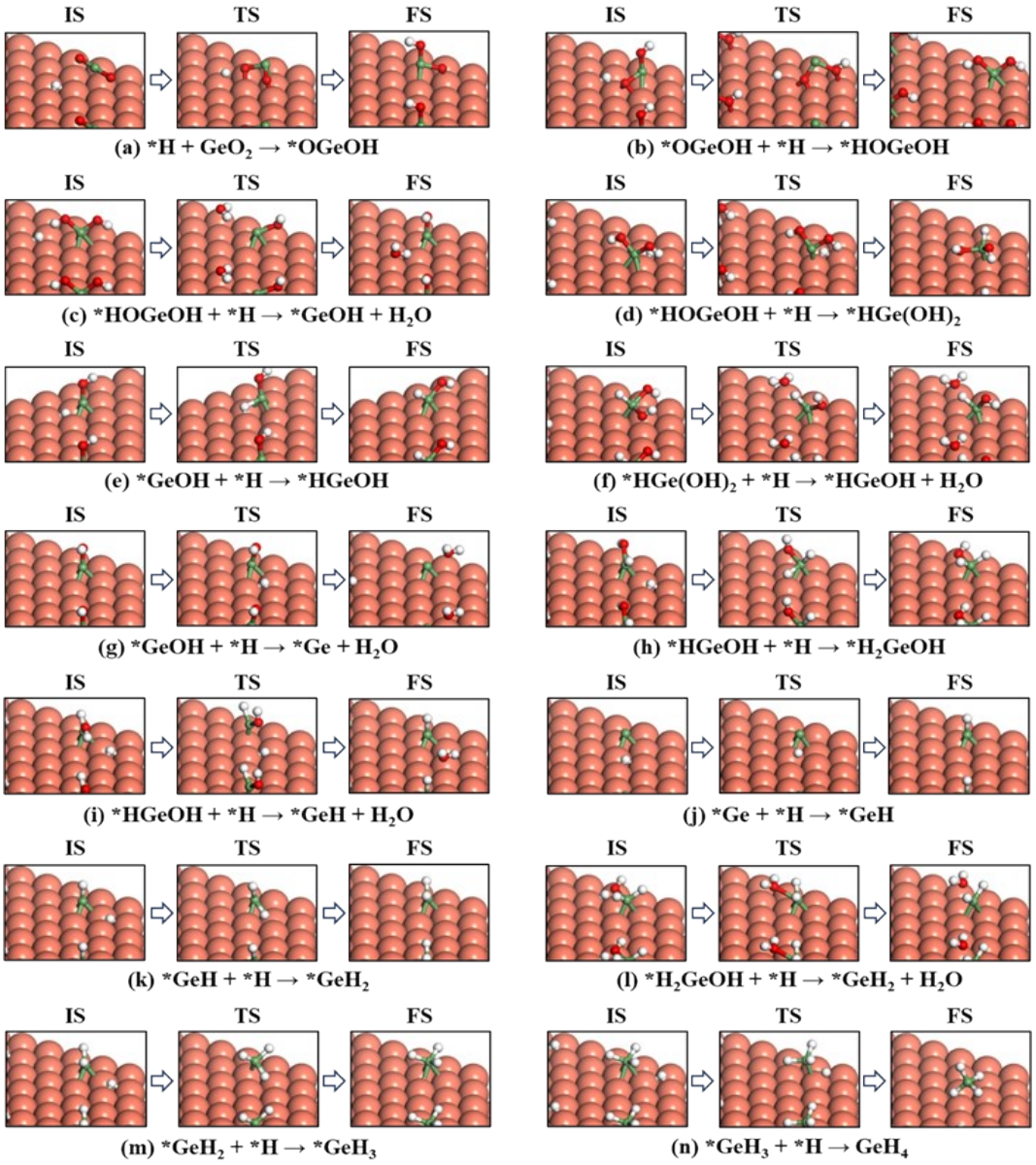

Figure S26. Structures of IS, TS and FS for all the calculated elementary reactions in Figure 4. (a)-(n) Germane is generated via the first non-hydrolytic reaction pathways D-T and A-T. The orange, red, white, and green balls represent Cu, O, H and Ge atoms, respectively.